

Effect of Al and Ag co-doping on the structural and optical properties of zinc oxide thin films

XIAOQIANG LUO¹, LINHUA XU^{1,2,*}, FENGLIN XIAN^{2,*}, HAISU QIAN¹, WEN WANG¹

¹*School of Physics and Optoelectronic Engineering, Nanjing University of Information Science and Technology, Nanjing 210044, China*

²*Optoelectronic Materials and Devices Laboratory, Nanjing University of Information Science and Technology, Nanjing 210044, China*

In view of the potential applications of Al-Ag co-doped ZnO materials in the fields of optoelectronic and microelectronic devices, in this work, we explored the influence of Al-Ag co-doping on the structure, morphology, bandgap and luminescent properties of ZnO films. ZnAg_xAl_yO ($y=Al/Zn=0, 0.005, 0.01, 0.015$ and 0.02 ; $x=Ag/Zn=0.005$) thin films were coated on glass substrates by a simple wet chemical method, namely the sol-gel method. The morphology, structure, composition and optical properties of the samples were analyzed by scanning probe microscopy, X-ray diffraction, energy dispersive spectroscopy, ultraviolet-visible absorption spectroscopy and photoluminescence, respectively. The results show that Al-Ag co-doping makes the grain size of ZnO decrease and the films surface become smoother. The c-axis orientation degree is decreased and the ultraviolet emission is weakened. However, within the range of doping concentration studied, Al-Ag co-doping has little effect on the optical bandgap of ZnO films. These results are compared with other reported experimental results about the influence of Al-Ag co-doping on ZnO thin films.

(Received July 12, 2021; accepted October 5, 2022)

Keywords: Zinc oxide, Al-Ag co-doping, Thin films, Optical bandgap, Photoluminescence, SPM

1. Introduction

Some metal-oxide semiconductors with good optical and electrical properties [1-8] such as titanium dioxide (TiO₂), cadmium oxide (CdO), tin oxide (SnO₂), zinc oxide (ZnO), etc. have been widely used in many fields. In order to improve the structural, electrical or optical properties, it is necessary to carry out doping for these metal-oxide semiconductor materials [9-11]. For example, Divya et al. [12] found that Ni doping improved the conductivity of SnO₂; Kumar et al. [13] reported that Mn-Fe co-doping increased the photoresponsivity and external quantum efficiency of CdO film, which made it a potential application in photodetectors; Kumar [14] found that Ni doping could improve the room temperature ferromagnetism of SnO₂ films; Komaraiah et al. [15] reported that Ag doping reduced the optical bandgap and ultraviolet emission intensity of TiO₂ film, but enhanced its photocatalytic activity.

Among numerous metal-oxide semiconductor materials, zinc oxide with wide bandgap has been attracting investigators' attention strongly in recent years. This is mainly due to its advantages such as non-toxicity, abundant raw materials, high electromechanical coupling coefficient, good piezoelectric performance and electrical conductivity. Since most zinc oxide films contain oxygen vacancies or zinc interstitials, this makes ZnO films usually show n-type conductivity. If the ZnO film is doped with an appropriate amount of Al or Ga ions, better n-type conductivity can be obtained [16, 17]. However, up to now, stable and reproducible P-type doping is still a big

challenge for ZnO. Ag is considered to be a potential element that can realize the P-type conductivity of ZnO. However, to make the Ag-doped ZnO film produce P-type conductivity, it is necessary to strictly control the deposition parameters and heat treatment conditions [18-20]. Some researchers have reported that dual-element doping including Ag may be an effective strategy to realize the P-type conductivity of ZnO [21, 22]. In fact, dual-element doping including Ag may not only realize the P-type conductivity of ZnO, but also play an important role in regulating other properties of ZnO. For example, Liu et al. [23] found that Ag-Co co-doping could greatly enhance the room temperature ferromagnetism of ZnO; Arivalagan et al. [24] found that the addition of ZnO nanoparticles co-doped with Al and Ag to the ethylene glycol-water mixture enhanced the thermal conductivity for the base fluid; Ravichandran et al. [25] found that Ag-F co-doping could improve the antibacterial efficiency of ZnO. Therefore, it is very important to explore the physical properties of dual-element (including Ag) doped ZnO materials. By consulting the literature, it can be known that there are few reports on the effect of Ag and Al co-doping on ZnO films [24, 26]. In this study, a low-cost wet chemical method was used to deposit Ag and aluminum co-doped zinc oxide films, and the effect of Ag-Al co-doping on the morphology and optical properties of ZnO films was systematically studied.

2. Experimental

The sol-gel method was used to prepare ZnO films co-doped with aluminum and silver. A precursor solution was prepared using zinc acetate as the zinc source, ethanol as the solvent, monoethanolamine as the chelating agent, and aluminum nitrate and silver nitrate as the dopants. In the synthesized precursor solution, the concentration of zinc acetate was equal to 0.35 mol/L. After the precursor solution had been aged for 24 h at room temperature, we spread the precursor solution evenly on the glass substrate by a spin-coater, then dried the substrate with the precursor under an infrared lamp for 3 min, and then put it in a muffle furnace at 300 °C for 3 min for preheating treatment. We repeated the above process 10 times. Finally, the sample was annealed at 500 °C for one hour. The sample names and corresponding doping concentrations are shown in Table 1.

X-ray diffractometer (Bruker D8 Advance) was applied to analyze the structural properties of ZnO films. The microscopic morphology of the samples was analyzed by a scanning probe microscope (CSPM4000); the scanning mode was contact mode; the scanning area was 4 μm ×4 μm . The content of Al and Ag was determined by energy dispersive spectrometer (EDS). The absorption spectra of the samples were measured by an ultraviolet-visible spectrophotometer (TU-1901). The photoluminescence was used to study the luminescence behavior of the samples excited by UV light (325 nm).

3. Results and discussion

3.1. Changes in the structure and morphology of ZnO films caused by Ag-Al co-doping

The X-ray diffraction patterns shown in Fig. 1 reveal that all samples have crystallized into a hexagonal wurtzite structure (JCPDS No. 36-1451). On these patterns, except for a upright (002) diffraction peak, no diffraction peaks derived from other phases are observed. Compared with the undoped ZnO film, the intensity of the (002) diffraction peaks of the Ag-Al co-doped samples is reduced, while the full-width at half maximum of the diffraction peaks is increased. This indicates that although Ag-Al co-doping does not change the preferred orientation of the ZnO film along the c-axis, it reduces the crystalline quality and c-axis orientation degree of the film. Similar

results were also reported by Khan et al. [26]. However, the non-doped and Ag-Al co-doped ZnO films prepared by Khan et al. [26] were all randomly oriented. This may be mainly because they used diethanolamine as a sol stabilizer [27].

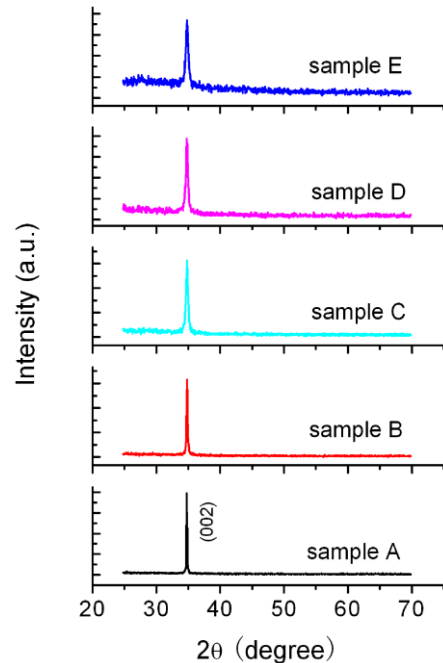


Fig. 1. XRD patterns of the samples (color online)

In the Ag-Al co-doped ZnO films fabricated by magnetron sputtering, Chen et al. [28] observed that Ag-Al co-doping greatly improved the c-axis orientation and crystal quality of the ZnO film (The FWHM of the (002) diffraction peak was greatly reduced). The doping concentration of Ag and Al is an important factor affecting the ZnO films, but Chen et al. did not give a specific doping concentration. Therefore, it is impossible for others to speculate the reason for the improvement of c-axis orientation and crystalline quality of Ag-Al co-doped ZnO films. In addition, the film deposition methods, deposition parameters, post-annealing treatment, etc. also greatly affect the growth orientation and crystalline quality of the Ag-Al co-doped ZnO films, and further affect the optical and electrical properties.

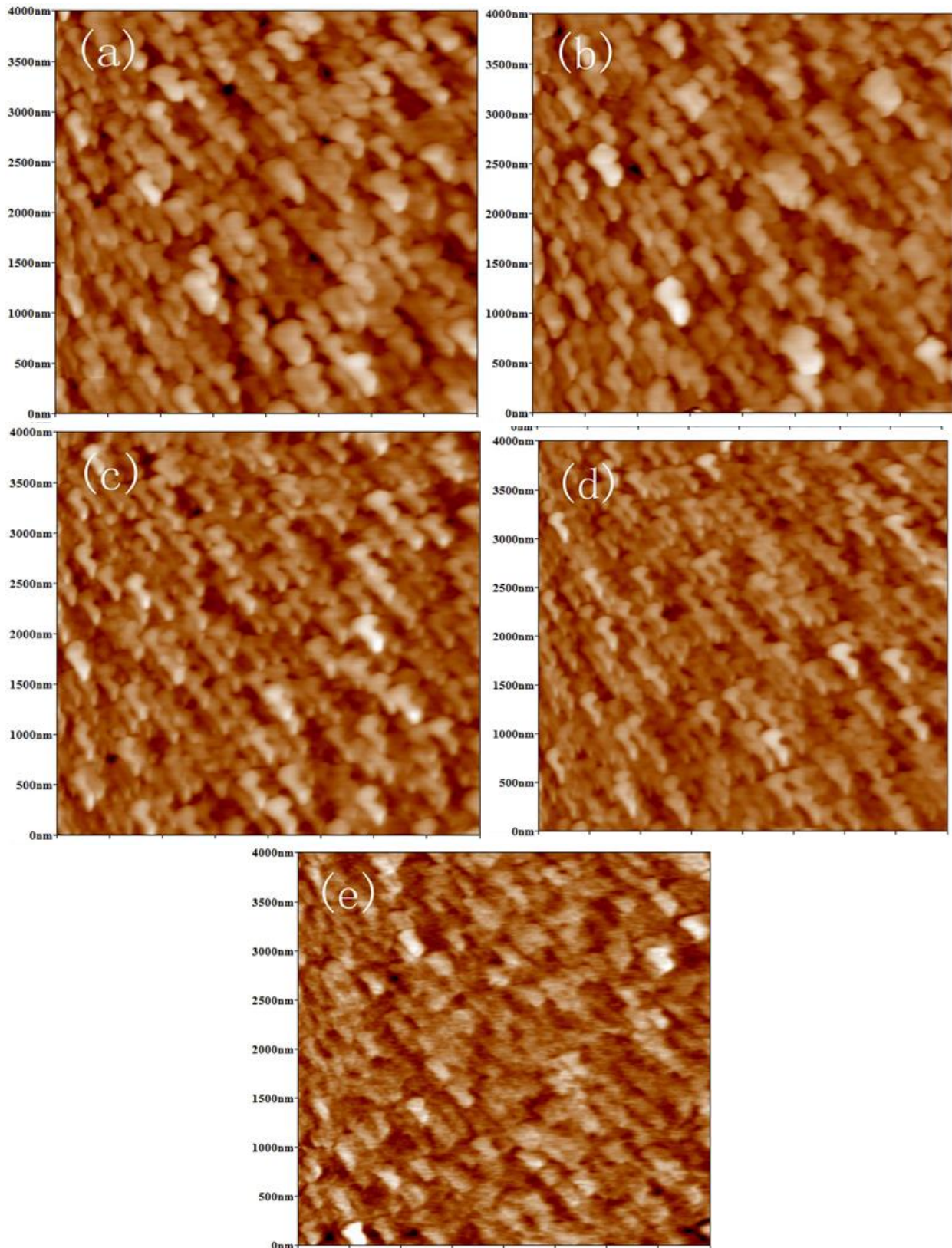


Fig. 2. SPM images of sample A (a), B (b), C (c), D (d) and E (e) (color online)

Fig. 2 shows the surface morphology of the Ag-Al co-doped ZnO films observed by the scanning probe microscope. A similar morphology was also observed by Ma et al. on ZnO films fabricated by PLD [29]. With the

increase of the Al doping level, the grains in the Ag-Al co-doped ZnO film are significantly reduced and the surface becomes smoother. The root-mean-square (RMS) roughness values of samples A, B, C, D and E are 3.38,

3.34, 3.27, 2.75 and 2.01 nm, respectively. That Al doping caused the grain size of ZnO films to decrease and the surface become smoother has also been reported in other papers [30]. Gómez-Pozos et al. [30] believe that this is because as the Al-doping concentration increases, some Al atoms segregate at the grain boundaries, preventing grain growth. In fact, with the increase of Al-doping concentration, the lattice distortions caused by the different radius between aluminum ion and zinc ion will also affect the growth of ZnO grains. For the Ag-Al co-doped ZnO films prepared by Khan et al. [26], they were found that with the increase of the Ag doping concentration, the grain size of the ZnO film first decreased, and then gradually increased. The different changing trends of grain size in ZnO films are closely related to different deposition conditions and post-annealing treatments.

In order to know the components in the samples, we chose sample E as a representative to test its energy dispersive spectrum, as shown in Fig. 3. In addition to Zn, O, Ag, and Al, other signals on this spectrum come from the glass substrate. Quantitative analysis shows that the atomic percentages of Ag and Al relative to Zn are 0.46% and 1.88%, respectively, which are close to the ratios in the precursor solution. Fig. 4 shows the mapping images

of different elements, from which we can see that both Ag and Al are evenly distributed in the ZnO film.

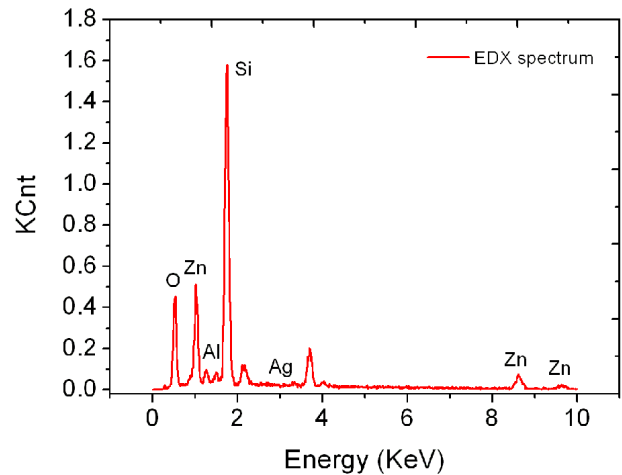


Fig. 3 EDS spectrum of the sample E (color online)

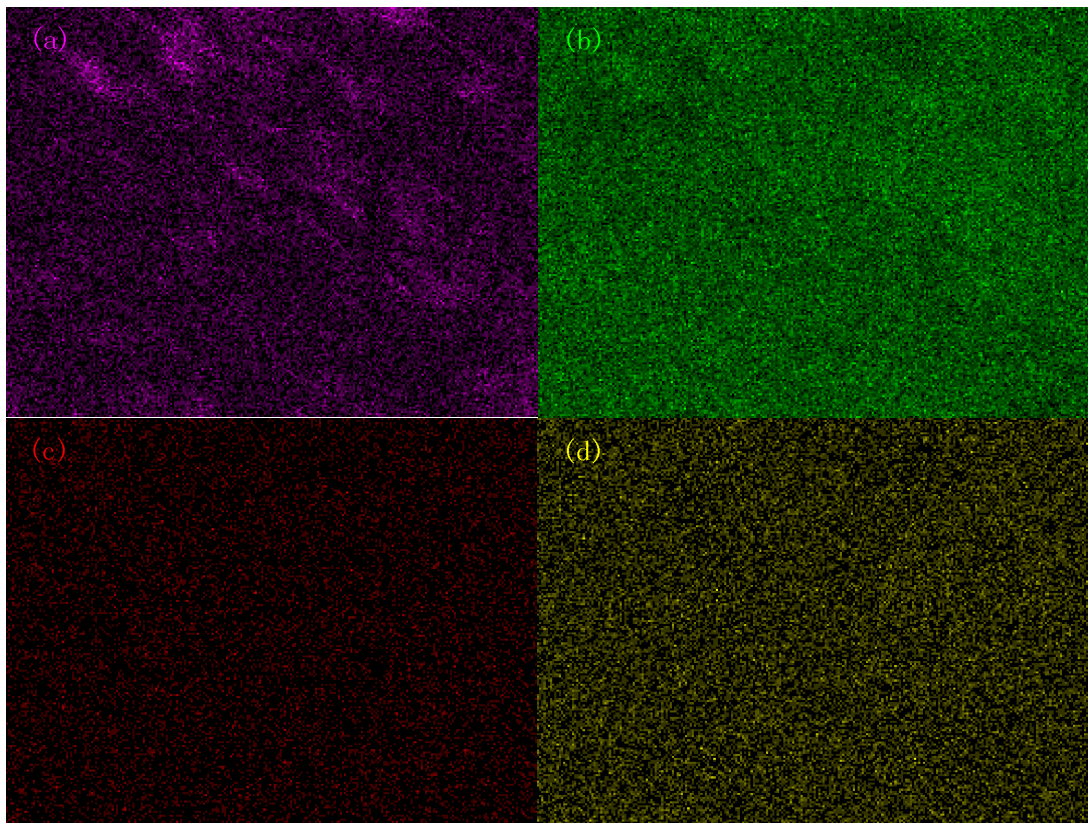


Fig. 4. Elemental mapping images of the representative sample E: (a) Zn, (b) O, (c) Ag and (d) Al (color online)

3.2. Changes in optical properties of ZnO films caused by Ag-Al co-doping

Fig. 5(a) gives the absorption spectra of the samples: all Ag-Al co-doped ZnO films have little absorption in the

visible region but strong absorption in the ultraviolet region and their absorption edges are located at about ~ 375 nm. Khan et al. [26] found that the Ag-Al co-doped ZnO films they prepared had a strong absorption peak at ~ 420 nm; as the Ag-doping concentration increased, this

absorption peak gradually enhanced and a red-shift of the peak appeared. Khan et al. [26] believe that this absorption peak is caused by the transition of electrons from the Ag_{Zn} energy level to the conduction band. However, similar absorption peaks are rarely reported in Ag ion doped ZnO. Taking into account that the Ag-Al co-doped ZnO film prepared by Khan et al. was annealed twice at 600 °C and the characteristics of this absorption peak, we deem that the absorption peak at ~ 420 nm is due to the surface plasmon resonance absorption caused by Ag nanoparticles [31]. This means that even for Ag-Al co-doping, the Ag-doping concentration and annealing temperature should be carefully controlled in order to make Ag ions enter ZnO lattices to replace Zn ions. The optical bandgaps have been estimated from the Tauc-relation [29], as shown in Fig. 5(b). Although the bandgap of the Ag-Al co-doped ZnO film increases with the rise of Al-doping

concentration, the magnitude of the change is small. For sample A, its band gap is 3.274 eV; for sample E, its band gap is 3.285 eV. Khan et al. [26] reported a similar trend of bandgap variation, and the bandgap variation amplitude was less than or equal to 0.02 eV. However, Chen et al. [28] found that the bandgap of ZnO films decreased from 3.273 eV to 3.254 eV after Ag-Al co-doping. From the above results, it can be seen that no matter the Ag-Al co-doping causes the bandgap of the ZnO film to increase or decrease, the magnitude of the change in bandgap is small. This may be due to the fact that both the doped Ag and Al ions enter the ZnO lattices and generate excess holes and electrons, respectively. However, compared with the undoped ZnO, the total carrier concentration is not significantly increased, so there is no significant impact on the bandgap.

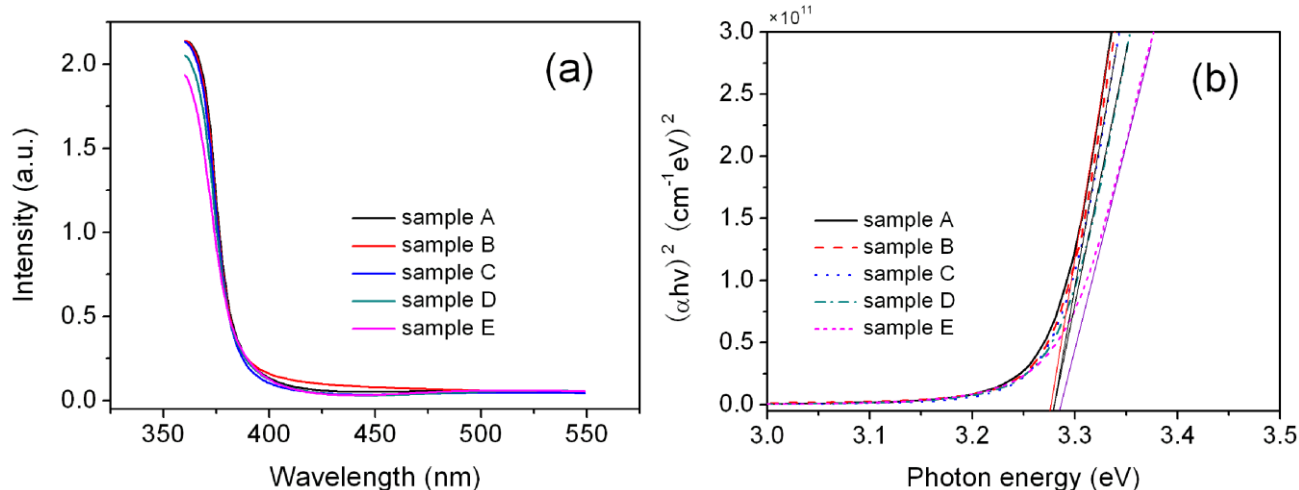


Fig. 5 (a) Absorption spectra and (b) bandgaps of the samples (color online)

The luminescent behavior of ZnO has always been the focus of researchers. Fig. 6 displays the photoluminescence spectra of undoped and Ag-Al co-doped ZnO films recorded at room temperature. All samples show an ultraviolet emission peak at 381 nm, which is believed to be caused by the recombination of excitons near the band edge. A similar UV emission peak also appeared in the Ag-Al co-doped ZnO film prepared by Khan et al. [26], although the excitation wavelength used by Khan et al. is different from the excitation wavelength we used. This indicates that the ultraviolet emission peak near 381 nm is the intrinsic emission of zinc oxide, and is not affected by the excitation wavelength within a certain excitation wavelength range. It can be seen from Fig. 6 that the Ag-Al co-doping makes the ultraviolet emission of the ZnO film greatly reduced, while the visible emission is relatively enhanced. This may be due to the increase in non-radiative recombination centers caused by doping. The reduction of UV emission of ZnO films caused by co-doping has also been reported by other researchers [32].

However, Chen et al. [28] found that the ZnO films deposited by magnetron sputtering, whether undoped or Ag-Al co-doped, have almost no ultraviolet emission but strong violet emission centered at 421 nm. Compared with pure ZnO films, the violet emission of Ag-Al co-doped ZnO films is enhanced and the visible emission band is broadened; the whole emission spectrum is superimposed by the emission bands centered at 421 nm, 468 nm, 508 nm and 550 nm, respectively. These visible emissions are all related to defects in ZnO such as V_{O} (oxygen vacancies) and Zn_{i} (zinc interstitials). Enhancement of visible emission intensity and broadening of emission band imply that Ag-Al co-doping may increase the density of point defects in ZnO films deposited by Chen et al. It can be seen from the above results that the preparation technology and deposition conditions of the ZnO films put a great influence on the chemical state of Al and Ag in ZnO, and which in turn affects the luminescence behavior.

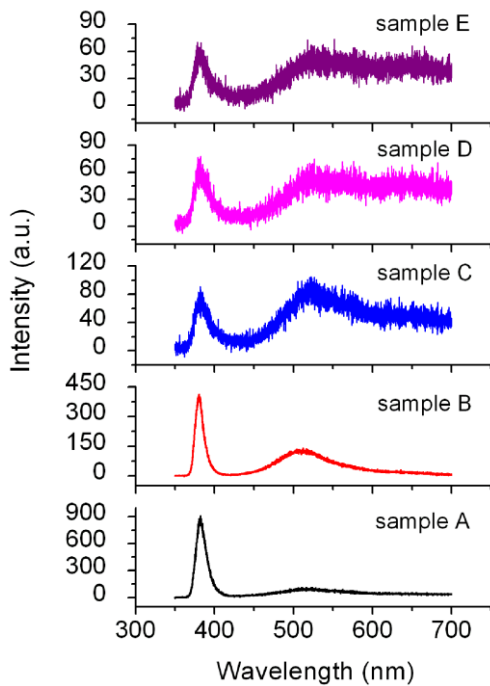


Fig. 6. Photoluminescence spectra of the samples (color online)

Table 1. Naming of ZnO thin films with different Al and Ag-doping concentrations

Sample name	Al-doping level (at.%)	Ag-doping level (at.%)
A	0	0
B	0.5	0.5
C	1.0	0.5
D	1.5	0.5
E	2.0	0.5

4. Conclusions

In this study, Ag-Al co-doped ZnO films were prepared by a low-cost wet chemical method. Compared with other reported experimental results about the effect of Al-Ag co-doping on ZnO thin films, we can see the similar results, such as the little effect of Al-Ag co-doping on the optical bandgap of ZnO thin films, and also see the divergent results, such as the effect of Al-Ag co-doping on the luminescence behavior of ZnO thin films. The difference of these experimental results is related to the chemical state of Al and Ag in ZnO films, which is related to film deposition methods, deposition parameters, doping concentrations, annealing temperatures and other factors. There are very few reports about Al-Ag co-doped ZnO films up to now. Therefore, in order to more understand the influence of Al-Ag co-doping on ZnO, more follow-up studies are needed.

Acknowledgements

This work is supported by the Innovation and Entrepreneurship Training Program for College Students

in 2021 (Grant no. XJDCZX202110300062) in Nanjing University of Information Science and Technology and the Natural Science Foundation of Jiangsu Province in China (Grant no. BK 20180784).

References

- [1] E. Muchuweni, T. S. Sathiaraj, M. T. Magama, P. Dzomba, *J. Optoelectron. Adv. M.* **22**(3-4), 200 (2020).
- [2] R. M. Mohamed, Z. I. Zaki, *J. Environ. Chem. Eng.* **9**, 104732 (2021).
- [3] J. Su, Q. Niu, R. Sun, X. An, Y. Zhang, *J. Optoelectron. Adv. M.* **20**(7-8), 441 (2018).
- [4] Q. Fu, J. Peng, Z. Yao, H. Zhao, Z. Ma, H. Tao, Y. Tu, Y. Tian, D. Zhou, Y. Han, *Appl. Surf. Sci.* **527**, 146923 (2020).
- [5] H. Akbari, Y. Azizian-Kalanderagh, *J. Optoelectron. Adv. M.* **20**(3-4), 175 (2018).
- [6] M. Soyulu, *Optik* **216**, 164865 (2020).
- [7] S. R. Alharbi, A. F. Qasrawi, *Physica E* **125**, 114386 (2021).
- [8] L. Soussi, T. Garmim, O. Karzazi, A. Rmili, A. E. Bachiri, A. Louardi, H. Erguig, *Surf. Interface* **19**, 100467 (2020).
- [9] L. T. T. Giang, N. T. T. Kieu, C. M. Tri, C. T. M. Dung, L. V. Hieu, L. Q. Vinh, D. M. Chien, T. D. Chinh, T. T. T. Van, *J. Lumin.* **228**, 117624 (2020).
- [10] K. Benzouai, M. Mahtali, Z. Daas, A. Bouabellou, *Optik* **229**, 166270 (2021).
- [11] A. A. Dakhel, *Mater. Chem. Phys.* **252**, 123163 (2020).
- [12] J. Divya, A. Pramothkumar, S. J. Gnanamuthu, D. C. B. Victoria, P. C. J. Prabakar, *Physica B* **588**, 412169 (2020).
- [13] S. Kumar, *Vacuum* **182**, 109725 (2020).
- [14] B. R. Kumar, K. H. Prasad, K. Kasirajan, M. Karunakaran, V. Ganesh, Y. Bitla, S. AlFaify, I. S. Yahia, *Sensors and Actuators A* **319**, 112544 (2021).
- [15] D. Komaraiah, E. Radha, J. Sivakumar, M. V. Ramana Reddy, R. Sayanna, *Opt. Mater.* **108**, 110401 (2020).
- [16] J. Lee, B. Park, *Thin Solid Films* **426**, 94 (2003).
- [17] Q. Ma, Z. Ye, H. He, S. Hu, J. Wang, L. Zhu, Y. Zhang, B. Zhao, *J. Cryst. Growth* **304**, 64 (2007).
- [18] R. Deng, Y. Zou, H. Tang, *Physica B* **403**, 2004 (2008).
- [19] I. S. Kim, E. Jeong, D. Y. Kim, M. Kumar, S. Choi, *Appl. Surf. Sci.* **255**, 4011 (2009).
- [20] L. Duan, W. Gao, R. Chen, Z. Fu, *Solid State Communications* **145**, 479 (2008).
- [21] J. J. Ortega, A. A. Ortiz-Hernández, J. Berumen-Torres, R. Escobar-Galindo, V. H. Méndez-García, J. J. Araiza, *Mater. Lett.* **181**, 12 (2016).

- [22] S. Long, Y. Li, B. Yao, Z. Ding, Y. Xu, G. Yang, R. Deng, Z. Xiao, D. Zhao, Z. Zhang, L. Zhang, H. Zhao, *Thin Solid Films* **600**, 13 (2016).
- [23] Y. Liu, Q. Hou, S. Sha, Z. Xu, *Vacuum* **173**, 109127 (2020).
- [24] A. R. Arivalagan, V. Karthik, R. Ramji, P. G. Venkatakrishnan, *Materials Today: Proceedings* **27**, 2364 (2020).
- [25] K. Ravichandran, P. Sathish, S. Snega, K. Karthika, P. V. Rajkumar, K. Subha, B. Sakthivel, *Powder Technology* **274**, 250 (2015).
- [26] F. Khan, S. Baek, J. H. Kim, *J. Alloys Compd.* **682**, 232 (2016).
- [27] M. Ohyama, H. Kozuka, T. Yoko, S. Sakka, *Journal of the Ceramic Society of Japan* **104**, 296 (1996).
- [28] H. Chen, Y. Qu, L. Sun, J. Peng, J. Ding, *Physica E* **114**, 113602 (2019).
- [29] X. Ma, J. Zhang, J. Lu, Z. Ye, *Appl. Surf. Sci.* **257**, 1310 (2010).
- [30] H. Gómez-Pozos, A. Maldonado, M. de la L. Olvera, *Mater. Lett.* **61**, 1460 (2007).
- [31] M. H. Habibi, R. Sheibani, *J. Sol-Gel Sci. Technol.* **54**, 195 (2010).
- [32] J. Xu, S. Shi, X. Zhang, Y. Wang, M. Zhu, L. Li, *Mater. Sci. Semicond. Processing* **16**, 732 (2013).

*Corresponding authors: congyu3256@tom.com;
xfl@nuist.edu.cn